Performance Metrics for Small-Signal Stability Assessment of DC-Distributed Power-System-Architecture Comparisons

S.Vesti, J.A. Oliver, R. Prieto and J.A. Cobos

T. Suntio

Abstract— **The objective of this paper is to provide performance metrics for small-signal stability assessment of a given system architecture. The stability margins are stated utilizing a concept of maximum peak criteria (MPC) derived from the behavior of an impedance-based sensitivity function. For each minor-loop gain defined at every system interface, a single number to state the robustness of stability is provided based on the computed maximum value of the corresponding sensitivity function. In order to compare various power-architecture solutions in terms of stability, a parameter providing an overall measure of the whole system stability is required. The selected figure of merit is geometric average of each maximum peak value within the system. It provides a meaningful metrics for system comparisons: the best system in terms of robust stability is the one that minimizes this index. In addition, the largest peak value within the system interfaces is given thus detecting the weakest point of the system in terms of robustness.** [1]

I. INTRODUCTION

Optimized size, cost and high efficiency as well as fast time-to-market are general design objectives for DC-distributed power systems. Therefore, the utilized components are typically commercial and the amount of available DC-DC converters from various manufacturers is large. Thus in order to obtain the design goals, selection of proper components and their connections to form system architecture can be a complex and time-consuming task. To facilitate this problem, a tool to design and optimize distributed systems is developed based on the methodology presented in [1,2]. This tool provides optimized architectural solutions in terms of size, cost and efficiency. However, due to the utilized simple converter models [3,4], the stability is usually ignored.

For small-signal stability assessment, a two-port structure is used to create models for system components [5-8]. This network composes of transfer functions that capture the internal converter dynamics and are obtained using frequency response measurements [7,8] or time-domain identification methods [9]. The two-port modeling structure can be also used to represent system filters, both commercial [10] and design optimized [11], based on measurements and analytic expressions, respectively.

Traditionally, the stability is assessed based on minor-loop gain [12] and it is widely used in various interconnected systems covering different application areas [12]–[15]. This method utilizes the impedance-based minor-loop gain, that is a ratio of the source or upstream subsystem output impedance and the load or downstream subsystem input impedance. Stability exists if the minor-loop gain satisfies the Nyquist stability criterion. An alternative method to assess system stability is based on analyzing passivity of bus impedance [16, 17]. However, this method is not appropriate for the analysis of a distributed system consisting of commercial converters [18].

Stability margins indicate how close a stable system is to instability. Typically, certain gain (GM) and phase (PM) margins are guaranteed by applying a concept of forbidden region in the complex plane, out of which the minor-loop gain shall stay [19]–[21]. In this paper, a concept of maximum peak criteria (MPC) is applied to provide the least conservative margins for stability. It is a well known method in control engineering to state robust stability of a closed-loop system by using the closeness of the loop gain to the point -1 in the complex plane [22]. This minimum distance is also recommended to be considered in the control loop design for converters [23, 24].

The MPC concept is also applicable in the analysis of distributed systems to state the robustness of stability for a well defined minor-loop gain [25]. In [18], this method is applied for a systematic small-signal stability analysis to provide least conservative margins for stability. However, certain stability margin is defined for each minor-loop gain

within the system without providing information of the overall system stability.

The objective of this paper is to obtain performance metrics for the whole system small-signal stability analysis. Different options for this index are evaluated in order to determine the most appropriate. Geometric average, that combines the stability information of each interface to a meaningful index, is selected to describe the overall stability. This figure of merit characterizes the central tendency of the system stability margins and therefore it provides a good measure for the architecture comparisons. Additionally it is of interest to identify the worst-case interface, i.e. the largest peak value within the system interfaces to provide more information of the system robustness for the user. For this purpose, an infinite norm that detects the maximum value is used.

The rest of the paper is organized as follows: the optimization and design tool are briefly described in Section II as well as the applied modeling method for stability analysis. Section III explains the utilized MPC-concept to obtain the stability margins and describes different alternatives for the performance metrics. In Section IV architectural solutions based on commercial converters are compared according to the selected metrics. The conclusions are finally drawn in Section V.

II. Optimization Methodology

The optimization of distributed architecture is a complex task and the amount of possible ways to connect various system components can be excessive. Therefore, the objective of the optimization tool is to facilitate this problem by providing architectural solutions with good trade-offs between desired system features including stability. The developed tool is described here briefly as well as the utilized converter models for the stability analysis.

A. Developed Design Tool

The designed optimization tool for distributed architectures is based on complex optimization algorithms [1, 2]. In order to analyze large number of design options, simplified converter models considering only the static features, are utilized [3]. The tool contains a library of various commercial converter models from different manufacturers. These models are obtained based on the datasheet information.

In order to generate the architectural solutions, the user needs to provide the following specifications for the optimization tool:

- Source specification (System input voltage)
- Load specifications (number of loads and their static parameters, input voltage and maximum power)
- Library of commercial converter models

These requirements are illustrated in Fig. 1 showing the user interface of the optimization tool. Subsequent to specifying the static system parameters and the required loads the commercial converters, based on which the optimized architectures are generated, are selected from the converter library or modeled according to their datasheet information. Utilizing this information, the tool provides a set of optimized architectural solutions and the user can compare the options in terms of optimized size, cost and efficiency and select the most appropriate solution. In addition to these parameters, it is desired to provide a figure of merit to describe the stability of each architectural solution.

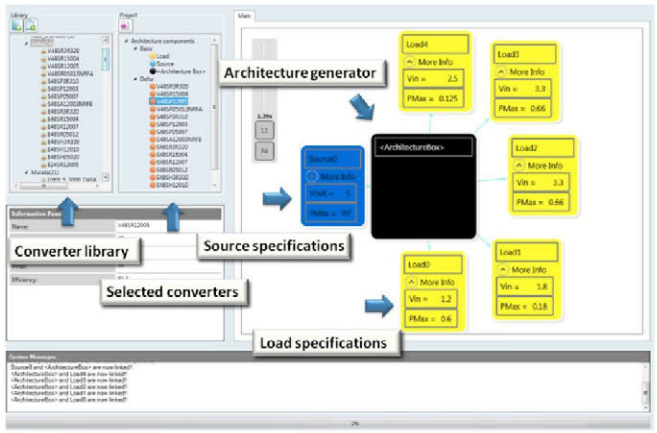

Fig. 1 User interface of the optimization tool.

B. Converter Models for Small-Signal Stability

In order to analyze the system stability, the transfer functions describing the converter dynamics are required and can be obtained as discussed in [7-9]. These transfer functions are given in (1) as a two-port network, shown in Fig. 2.

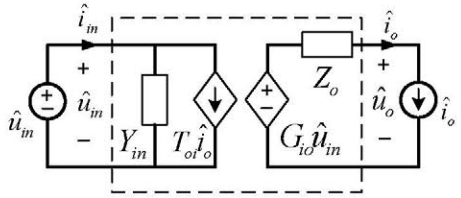

Fig. 2 Two-port structure of the converter with ideal source and load.

$$\begin{aligned}\hat{i}_{in} &= Y_{in}\hat{u}_{in} + T_{oi}\hat{i}_o \\ \hat{u}_o &= G_{io}\hat{u}_{in} - Z_o\hat{i}_o\end{aligned} \tag{1}$$

When the converters are interconnected to a system, adverse interactions might occur due to the converter sensitivity to the external impedances possibly leading to degraded performance or even instability. The influence of the source- or load-side impedance to the internal converter transfer functions in (1) is analyzed, as described in more detail in [25], providing the corresponding source and load-affected transfer functions according to (2) and (3), respectively.

$$\hat{i}_{in} = \frac{Y_{in}}{1+Z_sY_{in}}\hat{u}_{in} + \frac{T_{oi}}{1+Z_sY_{in}}\hat{i}_o$$
$$\hat{u}_o = \frac{G_{io}}{1+Z_sY_{in}}\hat{u}_{in} - \frac{1+Z_sY_{in-sco}}{1+Z_sY_{in}}Z_o\cdot\hat{i}_o$$
$$Y_{in-sco} = Y_{in} + \frac{G_{io}T_{oi}}{Z_o} \quad (2)$$

$$\hat{i}_{in} = \frac{1+Z_{o-oci}Y_L}{1+Z_oY_L}Y_{in}\cdot\hat{u}_{in} + \frac{T_{oi}}{1+Z_oY_L}\hat{i}_o$$
$$\hat{u}_o = \frac{G_{io}}{1+Z_oY_L}\cdot\hat{u}_{in} - \frac{Z_o}{1+Z_oY_L}\cdot\hat{i}_o$$
$$Z_{o-oci} = Z_o + \frac{G_{io}T_{oi}}{Y_{in}} \quad (3)$$

Based on (2) and (3), the minor-loop gains utilized for stability analysis are Z_sY_{in} for the source-side and Z_oY_L for the load-side. The stability is then assessed applying Nyquist stability criterion to these minor-loop gains. The robustness of system stability is analyzed based on the MPC- concept.

III. Performance Metrics for Small-Signal Stability

Stability analysis is desired to be integrated as a part of the developed optimization tool, described in the previous section. The objective is to provide a parameter for the whole system stability, in addition to the other optimized system features. By applying the MPC-concept, the least conservative stability margins are stated at each system interface. Based on this information, the performance metrics for the whole system stability is formed. This section first explains the method applied to obtain the stability margins and then describes the selection process for the system performance metrics.

A. Stability Margins

Stability margins are measures of how close a stable system is to instability. A good measure is the closeness of the loop gain to the point -1 in the complex plane. This minimum distance can be expressed as 1/Ms, the Ms is a peak value of a sensitivity function, defined in (4), where L denotes a loop gain. For a closed-loop system, the sensitivity function is used as a measure of robustness as well as the worst case performance degradation. The peak value of this function provides margins for robust stability according to (5) [22].

$$S = \frac{1}{1+L} \quad (4)$$

$$PM \geq 2\arcsin\left(\frac{1}{2|S_{\max}|}\right) \qquad GM \geq \frac{1}{1-1/|S_{\max}|} \quad (5)$$

To guarantee both robust stability and performance, the maximum peak of the sensitivity function is required to be small, typically less than 2 (6dB).

This concept can be used in distributed systems to provide margins for robust stability. The impedance-based minor-loop gain forms a similar sensitivity function (S) (6) as the loop gain L in (4) where the ML can be Z_sY_{in} or Z_oY_L for the source- and load-side minor-loop gains, respectively.

$$S = \frac{1}{1+ML} \quad (6)$$

In order to correctly predict robustness and provide the margins for distributed systems, the minor-loop gain is required to be determined at the interface closest to the direct input or output of the converter power stage as explicitly demonstrated in [25]. A large peak value indicates poor robustness i.e. low GM and PM and consequently, would cause peaking in the internal transfer functions according to (7) for source-affected converter.

$$\hat{i}_{in} = S\cdot Y_{in}\cdot\hat{u}_{ins} + S\cdot T_{oi}\cdot\hat{i}_o$$
$$\hat{u}_o = S\cdot G_{io}\cdot\hat{u}_{ins} - S\cdot(1+Z_sY_{in-sco})Z_o\cdot\hat{i}_o \quad (7)$$

The influence of the peaking is illustrated for a source-affected system by means of a commercial converter Texas PT78ST100. To emphasize the interactions, a large parasitic inductance is connected at the input of the converter to form excessive peak value of the corresponding sensitivity function. The influence of this peak to the converter output impedance is illustrated in Fig. 3, where the measured original, Z_o, (dashed line) and altered Z_{AL} (solid line) output impedances are shown.

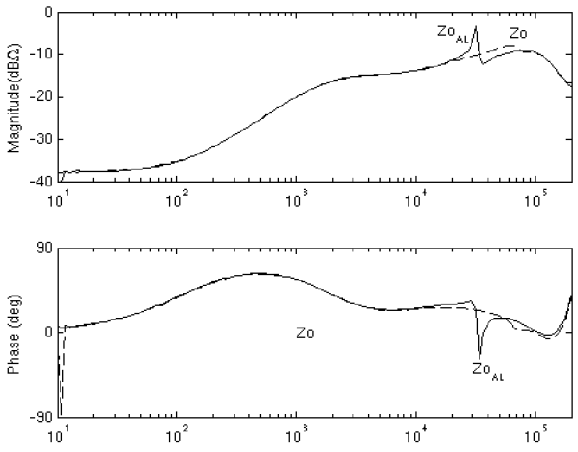

Fig. 3 Measured output impedance of PT78ST100 converter, dashed line is the internal output impedance and the solid line is the altered output impedance due to the excessive parasitic inductance.

The advantage of stating the stability margins utilizing the MPC concept is that a single parameter (value of the maximum peak) provides both, gain and phase margins.

These robust stability margins can be expressed also as a forbidden region in the complex plane. The highlighted circular area in Fig. 4 illustrates the MPC-based forbidden area [25], having the maximum peak of 2 (6dB) compared to the regions in [19-21]. This area occupies the minimum space in the complex plane thus providing the least conservative margins for stability guaranteeing robustness. With Ms = 2 the margins of GM ≥ 6dB and PM ≥ 29° are guaranteed. However, in addition to avoid intersecting the MPC-area, the Nyquist stability criterion must be complied.

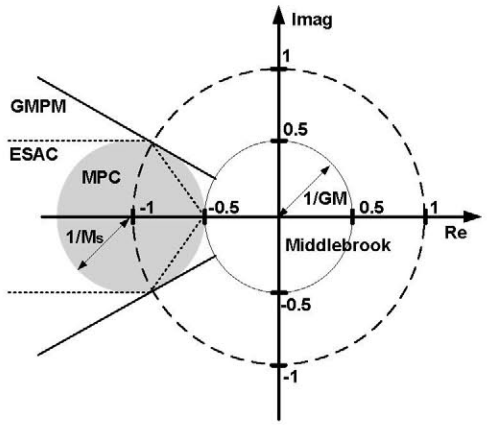

Fig. 4 The MPC-based forbidden region with the ESAC and GMPM regions.

B. System Stability Index

By applying the MPC-concept, the stability margins are stated as a one peak value for each interface within the system. For the stability margins presented in this paper, the maximum value is selected as 2, corresponding to a peaking of 6dB. Depending on the system requirements, stricter criteria regarding robustness might be needed and the peak value can be selected accordingly. Based on this information, a single number providing an overall measure of the stability is desired to be obtained.

In control theory, various norms are used to give a measure of the size of a vector, a matrix, a signal, or a system for synthesizing the controller. Most commonly used norms are H_2 and H_∞, defined in (8) [22].

$$H_2 = \sqrt{x_1^2 + x_2^2 \cdots x_n^2}$$
$$H_\infty = |x|_{\max} \tag{8}$$

The H_∞ norm detects the largest singular value, whereas the H_2 norm corresponds to a sum of the squares of all singular values. Applying the H_∞ norm to provide the stability index would only provide information of the system interface with the largest peak value ignoring the rest of the system. The H_2 norm would consider each singular value of the system interfaces. However, in order to obtain a meaningful number to state the stability, a weighting function would be needed to scale this value. Therefore, these norms are not the most appropriate ones to characterize the overall system stability.

In statistics a measure for central tendency of a set of numbers is provided applying different types of averages: arithmetic, geometric and harmonic defined in (9), respectively [26].

$$A.M. = \frac{x_1 + x_2 + \cdots + x_n}{n}$$
$$G.M. = \sqrt[n]{x_1 x_2 \cdots x_n}$$
$$H.M. = \frac{n}{\frac{1}{x_1} + \frac{1}{x_2} + \cdots \frac{1}{x_n}} \tag{9}$$

From the point of view of the whole system stability, a measure of the central tendency of all the peak values provides a meaningful metrics for the system comparisons. Table I illustrates the system stability index while applying the means defined in (9). The system consists of four interfaces and the maximum peak values Ms, at each interface are given for two different systems.

TABLE I. SYSTEM STABILITY INDEX APPLYING DIFFERENT MEANS.

	Ms value at each interface	A.M.	G.M.	H.M.
System 1	1.2; 1.3; 1.4; 1.2	1.275	1.272	1.269
System 2	1.1; 1.12; 2; 1.1	1.33	1.28	1.24

For System 1, the peak values for each interface are close and it can be observed that all the applied means provide similar stability index. However, for System 2 where one interface has a much higher peak value than the rest, more difference exists between the obtained average values.

The Arithmetic mean is, in general, the most frequently utilized. However, it is sensitive to large anomalies within the values and would not necessarily provide the most representative value for the overall system stability. The geometric and harmonic averages characterize better the typical values because they dampen the effect of very high or very low values. The geometric mean can be also expressed as the average of the logarithmic values of a set of numbers, converted back to a base 10 number as given in (10).

$$\log(\text{G.M.}) = \frac{\log x_1 + \log x_2 + \cdots + \log x_n}{n} \tag{10}$$

The peak value given for each interface is the inverse of the minimum distance between -1 and the minor-loop gain on the complex plane. It is often illustrative to express the peaking of the sensitivity function in dB especially when plotted in the frequency domain, even though the corresponding GM and PM are computed based on the absolute value according to (5). Thus the geometric average (9) of the absolute values of the maximum peaks is the arithmetic average of the corresponding peak values expressed in dB (10). The geometric average is, therefore,

considered to provide the most meaningful performance metrics for the system stability.

The best system in terms of robust stability is the one that minimizes the stability index. However, two systems with different peak values might have the same geometric average as illustrated in Table II for Systems 3 and 4.

TABLE II. COMPUTED GEOMETRIC AVERAGES FOR TWO SYSTEMS.

	Ms at each interface	G.M.
System 3	1.18; 1.2; 1.14; 2	1.34
System 4	1.4; 1.3;1.38; 1.3	1.34

It can be observed that for System 3 one peak value (Ms = 2) is close to violate the margins for robust stability whereas for System 4, the largest peak value provides good margins (Ms = 1.4). Therefore, it is of interest to detect the worst case interface and thus provide additional information regarding the system robustness to facilitate the architecture comparisons. The infinite norm (8) that captures the largest value within the set of numbers is applied to detect the weakest point of the system in terms of robustness in addition to the geometric average.

IV. EXPERIMENTAL VALIDATION

The objective of the selected performance metrics is to enable system comparisons in terms of robust stability. In this section, four state-of-the-art converters are utilized to form different architectures based on given system requirements. The obtained architectures are compared according to the selected performance metrics.

A. System comparisons

The static specifications for a simple distributed architecture are shown in Fig. 5. The loads are assumed ideal and only the required voltage level and maximum power are specified. The commercial converters utilized to generate the architectural solutions are:

- PT78ST100 Texas Instruments (U_{in}: 9-38V, U_o: 5V, P_{max}: 7.5W). Module number: M2
- TSR-1 Traco Power (U_{in}: 4.75-36V, U_o: 3.3V, P_{max}: 3.3W). Module number: M3
- LM2853 National Semiconductor (U_{in}: 5.5-3.3V, U_o: 3.3V, P_{max}: 9.9W). Module number: M4

Based on the given specifications, three different architectural solutions are obtained based on the utilized converters. Each structure contains a single stage input filter as shown in Fig. 6 with the following component values:

- F1 (L: 200µH, ESR_L: 100mΩ, C: 260µF, ESR_C: 100mΩ)
- F2 (L: 260µH, ESR_L: 160mΩ, C: 260µF, ESR_C: 100mΩ)
- F3 (L: 120µH, ESR_L: 160mΩ, C: 300µF, ESR_C: 100mΩ)

The different architectural structures are shown in Figs. 7 a), b) and c), where the converters are referred as the module numbers and the interfaces where the minor-loop gains for the stability analysis are defined, are emphasized and numbered.

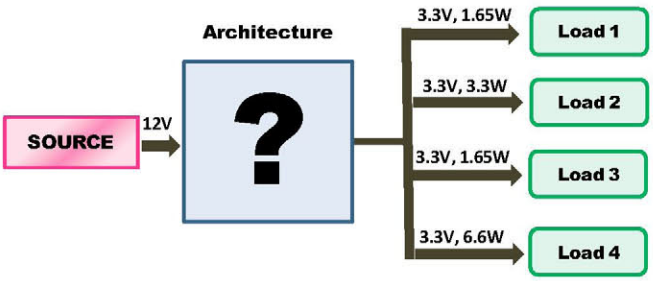

Fig. 5 Source and load specifications for system architecture.

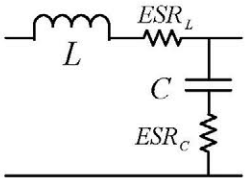

Fig. 6 Single stage input filter structure.

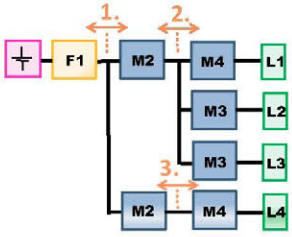

Fig.7 a) Architectural structure 1.

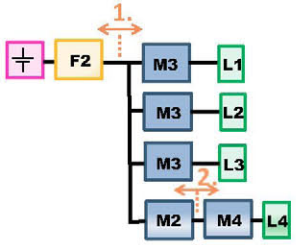

Fig.7 b) Architectural structure 2.

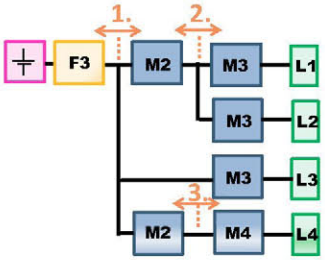

Fig.7 c) Architectural structure 3.

Frequency response measurements were performed to characterize each component at a specific operating point according to the system specifications. For instance, architectural structure 3 required that the input impedance of the module M3 (TSR-1 Traco Power) is measured at three different operating points while it is supplying the loads L1, L2 and L3 according to their needs. Fig. 8 shows these

impedances Zin_{L1} (U_{in}: 5V, I_o: 0.5A), Zin_{L2} (U_{in}: 5V, I_o: 1A) and Zin_{L3} (U_{in}: 12V, I_o: 0.5A).

Based on the obtained measurement data, the minor-loop gain based sensitivity functions can be computed according to (6) for each system interface. For the architectural structure 1, the computed sensitivity functions in decibels at the interfaces 1 (M_{s1}) and 2 (M_{s2}) are illustrated in Fig. 9. The first minor-loop gain, ML1 is formed between the filter output impedance and the parallel-connected input impedances of the modules M2 (U_{in}: 12V& I_o: 1.4A). The second minor-loop gain ML2, at the interface 2, consists of the module M2 (U_{in}: 12V & I_o: 1.4A) output impedance and the parallel-connected input impedances of the modules M3 (U_{in}: 5V, I_o: 0.5A) and M3 (U_{in}: 5V, I_o: 1A) as well as M4 (U_{in}: 5V, I_o: 0.5A). These minor-loop gains are shown in Fig. 10 with the MPC region, where the minimum distance between the point -1 and the minor-loop gain corresponds to the absolute value of the peak sensitivity function in Fig.9.

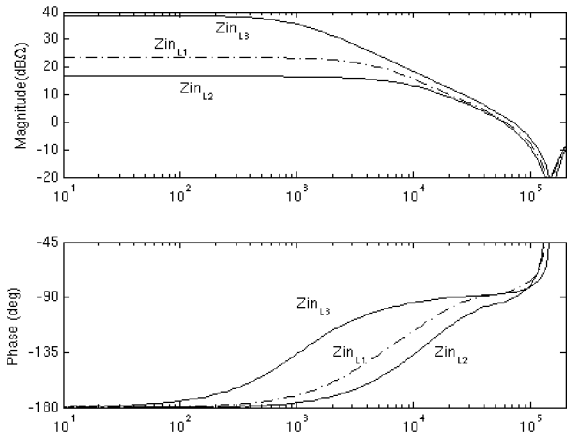

Fig. 8 The measured input impedances Zin_{L1}, Zin_{L2}, Zin_{L3} of the commercial module M3 at the operation points U_{in}: 5V & I_o: 0.5A, U_{in}: 5V & I_o: 1A and U_{in}: 12V & I_o: 0.5A, respectively for architecture 3.

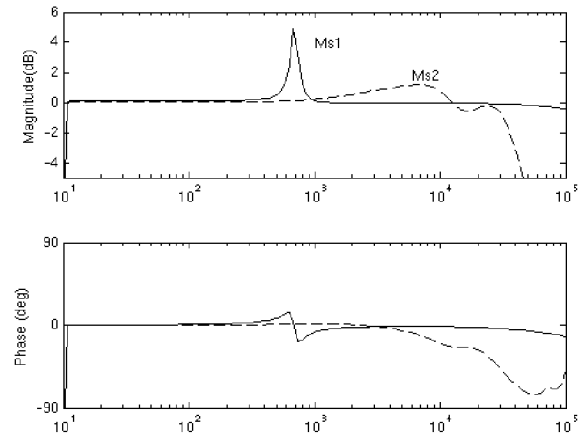

Fig. 9 Computed sensitivity functions, Ms1 (solid line) and Ms2 (dashed line) for architecture 1.

The computed peak values for each structure at every interface are shown in Table III in addition to the obtained performance metrics for stability. Based on the analysis, architectural structure 3 has the best stability index and the smallest worst case interface value as a comparison to the other solutions. By including the stability analysis to the optimization tool, the user can select the most appropriate architecture structure based on comparisons regarding the size, cost and efficiency as well as stability.

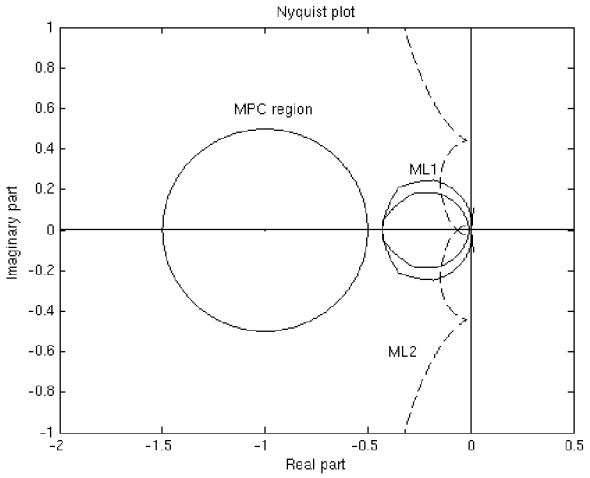

Fig. 10 Minor-loop gains at the interfaces 1 and 2 for architectural solution 1 with the MPC-region.

TABLE III. THE COMPUTED PEAK VALUES BASED ON MEASUREMENT DATA FOR EACH SYSTEM STRUCTURE.

Interface	Architecture 1	Architecture 2	Architecture 3
Ms 1	1.75	1.66	1.2
Ms 2	1.14	1.16	1.11
Ms 3	1.16	-	1.16
G.M.	**1.32**	**1.39**	**1.16**
H_∞	**1.75**	**1.66**	**1.2**

B. Discussions

The small example system with a simple input filter, containing only three interfaces was used to demonstrate the application of the selected performance metrics for stability. Nevertheless, this method is applicable also for more complex DC-distributed systems with more components. In certain applications, a distributed input filter solution is used for more optimized design and even though it is not analyzed in this paper, the stability can be assessed in a similar way representing every filter with the two-port model.

The utilized stability assessment method is operation-point dependent because it is a linear analysis implying that

each component needs to be characterized at a specific operation point. This operation point influences the stability margins. However, by characterizing the converters under different operating conditions, the stability index can be provided for each system at various operating conditions. The limitation of this linear method is that the system large-signal stability is not considered. Therefore, the presented analysis provides a necessary, but not sufficient condition for the global system stability.

By implementing this stability assessment method to the optimization tool, it provides the information whether the selected commercial components can be connected to form a system according to the defined specifications, guaranteeing stability and unaltered performance. In order to verify the system large-signal stability, which is more dependent on the specific system features such as protections and startup, further time-domain simulations are required.

V. CONCLUSIONS

The main objective of this paper is to present a simple metrics regarding the system small-signal stability, based on which different architectural solutions can be compared in terms of stability. The applied MPC-concept provides the least conservative method to obtain stability margins for one interface. Typically distributed systems consist of various interfaces. Therefore, it is important to obtain a single figure of merit to provide an overall measure of the whole system stability. The selected performance metrics for the small-signal stability is the geometric average of the peak values in each interface. It provides a meaningful metrics for system comparisons: the best system in terms of robust stability is the one that minimizes this index. Furthermore, the largest peak value within the system is given thus providing additional information regarding the system robustness and facilitating the system comparison by detecting the weakest point of the system in terms of robustness.

REFERENCES

[1] L. Laguna, R. Prieto, J. A. Oliver, J.A. Cobos, and H. Visairo-Cruz , "Fast architecture generation and evaluation techniques for the design of large power systems," in *Proc. IEEE ECCE, 2010, pp.3464-3469*.

[2] L. Laguna, R. Prieto,J. A. Oliver, J.A. Cobos, H Visairo,and P. Kumar, "Power conversion modeling methodology based on building block models," in *Proc. IEEE ECCE,* 2009, pp.3404-3410.

[3] J.A. Oliver, R. Prieto, V. Romero, and J.A Cobos, "Behavioral modeling of dc-dc converters for large signal simulation of distributed power systems," in *Proc. IEEE APEC*, 2006, pp. 6 pp. 19-23.

[4] R. Prieto, L. Laguna, J.A. Oliver, and J.A. Cobos, "DC/DC converter parametric models for system level simulation," in *Proc. IEEE APEC*, 2009, pp. 292-297.

[5] B. H. Cho, and F. C. Y. Lee, "Modeling and analysis of spacecraft power systems," *IEEE Trans. Power Electron.*, vol. 3, no. 1, pp. 44-54, Jan. 1988.

[6] C. C. Bilberry, M. S. Mazzola, and J. Gafford, "Power supply on chip (PwrSoC) model identification using black-box modeling techniques," in *Proc. IEEE APEC,* 2012, pp.1821-1825.

[7] L. Arnedo, R. Burgos, D. Boroyevich, F. Wang, "System-level black-box DC-to-DC converter models," in *Proc. IEEE APEC 2009,* pp.1476-1481.

[8] S. Vesti, J.A. Oliver, R. Prieto, J.A. Cobos, J. Huusari, T. Suntio, "Practical characterization of input-parallel-connected converters with a common input filter," in *Proc. IEEE APEC, 2012*, pp.1845-1852.

[9] V. Valdivia, A. Barrado, A.M. Roldan, C. Fernandez, and P. Zumel, "Black-box modeling of DC-DC converters based on transient response analysis and parametric identification methods," in *Proc. IEEE APEC, 2010,* pp.1131-1138.

[10] A. Hentunen, K. Zenger, and T. Suntio, "A systematic approach to analyze the stability of distributed power supply systems" in *Proc. Nordic Workshop on Power Electronics*, 2004, 6pp.

[11] N. Hensgens, J. Oliver, J.A. Cobos, S. Skibin, and A. Ecklebe, "Design and multi-objetive optimization of EMI input filters, " in *Proc. IEEE APEC, 2013*, pp.2506-2513.

[12] R. D. Middlebrook, "Input filter considerations in design and application of switching regulators," in *Proc. IEEE IAS*, 1976, pp. 336-382.

[13] B. Choi, D. Kim, D. Lee, S. Choi, and J. Sun, "Analysis of input filter interactions in switching power converters," *IEEE Trans. Power Electronon.,* vol. 22, no. 2, pp.452-460, Mar. 2007.

[14] Jian Sun; , "Impedance-based stability criterion for grid-connected inverters," *IEEE Trans. Power Electron.,* vol. 26, no. 11, pp.3075-3078, Nov. 2011.

[15] V. Valdivia, A. Lázaro, A. Barrado, P. Zumel, C. Fernández, M. Sanz, "Impedance Identification Procedure of Three-Phase Balanced Voltage Source Inverters Based on Transient Response Measurements," *IEEE Trans. Power Electron,* vol.26, no.12, pp.3810-3816, Dec. 2011.

[16] A. Riccobono, E. Santi, "A novel passivity-based stability criterion (PBSC) for switching converter DC distribution systems," in *Proc. IEEE APEC,* 2012, pp.2560-2567.

[17] A. Riccobono, E. Santi, "Comprehensive review of stability criteria for DC distribution systems," in *Proc. IEEE ECCE*, 2012, pp.3917-3925.

[18] S. Vesti, J.A. Oliver, R. Prieto, J.A. Cobos, T. Suntio, "Simplified small-signal stability analysis for optimized power system architecture," in *Proc. IEEE APEC, 2013*, pp. 1702-1708.

[19] S. D. Sudhoff, S. F. Glover, P. T. Lamm, D. H. Schmucker, and D. E. Delisle, 'Admittance space stability analysis of power electronic systems,' *IEEE Trans. Aerospace and Electron. Syst.*, vol. 36, no. 3, pp. 965-973, Jul. 2000.

[20] C. M. Wildrick, F. C. Lee, B. H. Cho, and B. Choi, 'A method of defining the load impedance specification for a stable distributed power system,' *IEEE Trans. Power Electron.*, vol. 10, no. 3, pp. 280-285, May 1995.

[21] X. Feng, J. Liu, and F. C. Lee 'Impedance specification for stable DC distributed power systems,' *IEEE Trans. Power Electron.*, vol. 17, no. 2, pp. 157-162, Mar. 2002.

[22] S. Skogestad, and I. Postlethwaite, *'Multivariable Feedback Control – Analysis and Design,'* Chichester, U.K., John Wiley and Sons, 1998, pp. 30-36.

[23] S. Sandler, "When bode plots fail us," *Power Electronics Technology,* vol. 38, no. 5, pp. 22, May 2012.

[24] C. Basso, "The dark side of loop control theory " tutorial *IEEE APEC 2012.*

[25] S. Vesti, T. Suntio, J. A. Oliver, R. Prieto, and J. A. Cobos, "Impedance-based stability and transient-performance assessment applying maximum peak criteria," *IEEE Trans. Power Electron.*, vol. 28, no. 5, pp. 2099-2104, May 2013.

[26] Zwillinger, D. (Ed.). *CRC Standard Mathematical Tables and Formulae.* Boca Raton, FL: CRC Press, 1995.